energy&fuels

Article

pubs.acs.org/EF

Hydrate-Based Methane Separation from the Drainage Coal-Bed Methane with Tetrahydrofuran Solution in the Presence of Sodium Dodecyl Sulfate

Xiao-Sen Li,*[,†,‡] Jing Cai,[†,‡] Zhao-Yang Chen,[†,‡] and Chun-Gang Xu[†,‡,§]

[†]Key Laboratory of Renewable Energy and Gas Hydrate, Guangzhou Institute of Energy Conversion, and [‡]Guangzhou Center for Gas Hydrate Research, Chinese Academy of Sciences, Guangzhou 510640, P. R. China

[§]Graduate University of Chinese Academy of Sciences, Beijing 100083, P. R. China

ABSTRACT: To determine the appropriate operating conditions for separating methane (CH_4) from drainage coal-bed methane (CBM) mixed with air, a hydrate-based methane separation method is proposed. The amount of gas uptake, CH_4 concentration in decomposed gas phase, CH_4 split fraction, and CH_4 separation factor are investigated at the initial operating pressure range of 1.50−4.50 MPa and 279.15 K in the presence of sodium dodecyl sulfate (SDS) with the concentration range of 0−1000 ppm in 1.0 mol % tetrahydrofuran (THF) aqueous solution. The results indicate that the 1.0 mol % THF aqueous solution with the addition of 300 ppm SDS at 2.50 MPa and 279.15 K is the optimal condition for recovering CH_4 from the drainage CBM via hydrate formation. Under the condition, the final amount of the gas uptake, the CH_4 concentration in decomposed gas phase, the CH_4 split fraction, and the CH_4 separation factor after a one-stage hydrate-based separation are up to 0.1364 mol, 69.93 mol %, 86.44%, and 10.77, respectively. The result illustrates that the hydrate-based CH_4 separation is a promising method to recover CH_4 from the drainage CBM at mild conditions. Moreover, CH_4 recovered from the drainage CBM can be directly utilized in industry.

1. INTRODUCTION

Coal-bed methane (CBM), mainly consisting of methane (CH_4), is a significant source of clean energy with a significant resources in China. The reserves of the CBM resource buried to a depth of 2000 m is more than 34 trillion cubic meters, ranking third in the world.[1] It exists in three forms in the coal seams: absorbed in the porous media, free in the fracture, and dissolving in the underwater of coal bed.[2] Thus, there are two principles to exploit CBM, such as discharging water[3,4] and replacing with carbon dioxide (CO_2).[5] Due to the complicated coal seam occurrence conditions, reservoir geological conditions, coal distribution, etc., discharging water is most widely applied to collect CBM through the extraction system of coal mines.[6] Accordingly, the exploited CBM is called drainage CBM with a low and unstable concentration of CH_4 mixed with air. Consequently, such drawbacks lead to the difficulties and risks for the subsequent processes of disposing the drainage CBM. Thus, the drainage CBM can only be emitted into the atmosphere to ensure the safety of coal mining. As a result, a large amount of potential clean resources are wasted, and the environment is contaminated. In China, the amount of CBM discharged into the atmosphere is approximately 1.94 billion cubic meters per year, ranking first in the world.[7] Therefore, it is necessary to undertake research on separating and recovering CH_4 from the drainage CBM.

However, the CH_4 concentration in drainage CBM is as low as 15−60 mol % and can even be lower than 15 mol %.[8] Drainage CBM can not be utilized directly in industry as natural gas unless the CH_4 concentration in the CBM is higher than 90 mol %. After the pretreatments of sulfur removal, desiccation, and deoxygenation, the drainage CBM mainly contains CH_4 and N_2. Consequently, the recovery of CH_4 from the drainage CBM is focused on the separation of CH_4 from the CH_4/N_2 gas mixture. At present, the technologies of separating the CH_4/N_2 gas mixture contain cryogenic fractionation, pressure swing absorption, and membrane separation. However, those technologies can not recover CH_4 from the drainage CBM effectively due to the limitations of cost and security on facility and operating process.[9] For example, the cryogenic fractionation technology can not ensure the stable operating condition for the variation of the CH_4 concentration in the drainage CBM, which requires changing the refrigerant composition to obtain a better CH_4 separation efficiency. The pressure swing absorption technology can not achieve a high CH_4 separation efficiency for the limitation of the absorbent, which has a close separation factor and little difference in absorbing capacity between CH_4 and N_2. Although the membrane separation technology has the advantage of simple craft and easy operation, it requires a huge cost of membrane materials. The above traditional gas separation technologies are not utilized widely in the industry to concentrate CH_4 from the drainage CBM. Therefore, an alterative safe and efficient way is required to recover CH_4 from the drainage CBM simulation gas (the CH_4/N_2 gas mixture). The hydrate-based separation is a potential technology to achieve the separation purpose.

The basis of the hydrate-based separation is the selective partition of the target component between the hydrate phase and the gaseous phase. Recently, the hydrate-based separation technology is generally applied to recover CO_2 from flue and

Received: November 17, 2011
Revised: January 18, 2012
Published: January 25, 2012

dx.doi.org/10.1021/ef201804d | *Energy Fuels* 2012, 26, 1144−1151

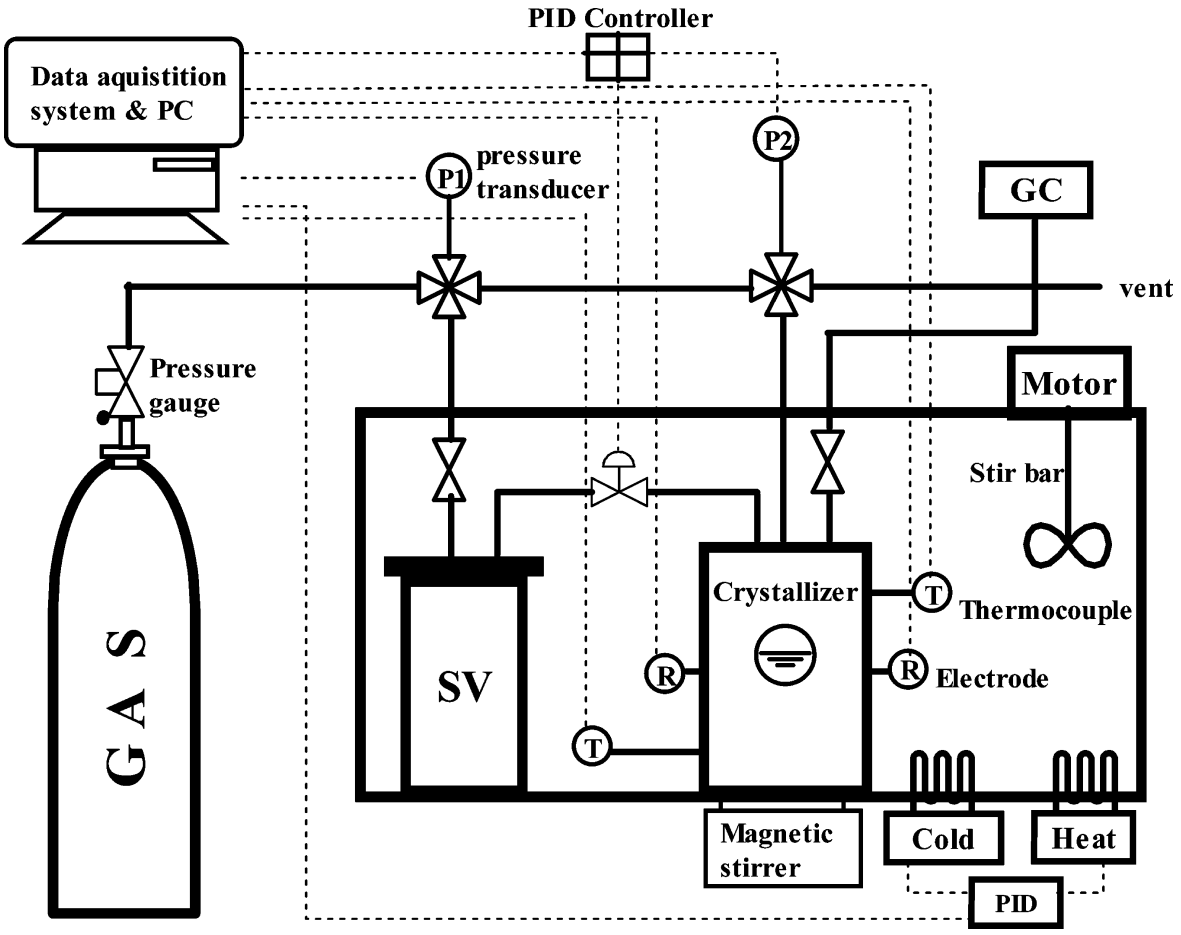

Figure 1. Experimental apparatus: CR, crystallizer; SV, supply vessel; T, thermo probe; P1 and P2, pressure transducers; R, resistance transducer; and GC, gas chromatographer.

fuel gas.[10−18] However, little is known about recovering CH_4 from the CH_4/N_2 gas mixture. Happel et al.[19] first proposed the different equilibrium conditions of the hydrate formation. Recently, the hydrate-based separation technology was adopted in the recovery of CH_4 from the CBM resource.[20−26] According to literature, the hydrate formation pressure of CH_4, N_2, and the CH_4/N_2 gas mixture with 50.25 mol % CH_4 are 5.02, 28.29, and 6.13 MPa, respectively, in the pure water system at a constant temperature (approximately 279.15 K).[27−29] Hence, the CH_4 hydrate can be formed more easily than the N_2 hydrate by controlling the operating pressure at the constant temperature.

However, the hydrate formation rate, the amount of the gas uptake, and the CH_4 separation efficiency are key factors which determine the application of the hydrate-based CH_4 separation technology in industry. Furthermore, in the pure water system, the hydrate formation pressure of the CH_4/N_2 gas mixture is too high to engender huge equipment and operating costs for the application of the hydrate-based separation in industry and the hydrate formation rate is too low to achieve large scale gas separation. In order to effectually lower the hydrate formation pressure and improve hydrate formation rate, the amount of the gas uptake, and the CH_4 separation efficiency, the hydrate formation additives or promoters, such as tetrahydrofuran (THF), sodium dodecyl sulfate (SDS), and tetrabutylammonium bromide (TBAB) are added in the separation processes. The formation pressure of the CH_4 and N_2 hydrate sharply drops in the systems with THF but the amount of the gas uptake and the CH_4 separation efficiency obviously decrease as well.[21,22] However, Zhang et al.[22] demonstrated that methane can be directly separated from the methane, nitrogen, and oxygen gas mixture via hydrate formation in the tetrahydrofuran solution without the pretreatments of deoxygenation. Nevertheless, the formation pressure of the CH_4 and N_2 hydrate is quite high in the SDS solution[21] and the CH_4 separation efficiency is only improved up to approximately 50% in the TBAB solution in the presence of SDS.[23] Therefore, the above hydrate formation systems are not available to recover CH_4 from the drainage CBM efficiently and reduce the cost in industrial application. Thus, it is necessary to study a new system to increase the hydrate formation rate, the amount of the gas uptake, and the CH_4 separation efficiency.

In this work, THF and SDS are adopted as the mixture promoter. Effects of the additions of the SDS with the different concentrations in 1.0 mol % THF aqueous solution and the different initial operating pressures on the hydrate formation rate, the amount of the gas uptake, the CH_4 concentration in the decomposed gas phase, the CH_4 split fraction, and the CH_4 separation factor were investigated. The purpose is to find the optimal condition for recovering CH_4 from the drainage CBM.

2. MATERIALS AND METHODS

2.1. Apparatus. Figure 1 shows the schematic of the experimental apparatus.[12] It consists of a supply vessel (SV) and a high hydrate crystallizer (CR) made of 316 stainless steel. The CR with an effective volume of 336 mL and the SV with the maximum volume of 1250 mL

dx.doi.org/10.1021/ef201804d | Energy Fuels 2012, 26, 1144−1151

Table 1. Experimental Conditions along with Composition Analysis and Separation Efficiencies for Different Systems

runs	system	T (K)	P (MPa)	concentration in residual gas phase (mol %) CH_4	concentration in residual gas phase (mol %) N_2	concentration in decomposed gas phase (mol %) CH_4	concentration in decomposed gas phase (mol %) N_2	gas uptake (mol)	S.Fr.	S.F.	t_i[a] (min)	V[b] (mol/min) × 10^{-3}
1	1.0 mol % THF	279.15	3.50	47.37	52.63	58.09	41.91	0.1490	0.7218	2.38	8.5	1.43
2	1.0 mol % THF + 250 ppm SDS	279.15	3.50	42.10	57.90	66.40	33.60	0.1632	0.6183	3.56	5.2	1.29
3	1.0 mol % THF + 300 ppm SDS[c]	279.15	3.50	46.06	53.94	58.78	44.22	0.1501	0.7757	2.17	7.2	1.65
4	1.0 mol % THF + 300 ppm SDS	279.15	3.50	45.61	54.39	65.73	41.27	0.1682	0.8187	3.34	2.3	1.39
5	1.0 mol % THF + 500 ppm SDS	279.15	3.50	45.24	54.76	65.17	34.83	0.1454	0.6880	3.79	1.6	1.97
6	1.0 mol % THF + 1000 ppm SDS	279.15	3.50	41.68	58.32	71.19	29.81	0.1185	0.7732	7.49	1.5	1.14
7	1.0 mol % THF + 300 ppm SDS	279.15	1.50	38.43	61.57	70.59	29.41	0.0808	0.9005	15.08	42	0.44
8	1.0 mol % THF + 300 ppm SDS	279.15	2.50	39.46	60.54	69.93	30.07	0.1364	0.8644	10.77	9.5	1.11
9	1.0 mol % THF + 300 ppm SDS	279.15	4.50	45.23	54.77	64.35	35.65	0.1636	0.6908	3.60	1.4	1.49

[a]Induction time. [b]CH_4–N_2 gas hydrate formation rates for 1 h after nucleation.[14,38] [c]Fresh water

are located inside the temperature-controlled water bath. The CR contains two visible windows to observe the process of hydrate formation. The contents in the CR are agitated by a magnetic stirrer (0–1000 rpm). The pressure in the CR and SV is measured using a MBS3000 absolute pressure transducer (0–25 MPa) with ±0.02 MPa accuracy. The temperature in the CR is measured using a Pt1000 thermo probe (JM6081) with the uncertainty of ±0.1 K. The signals of the pressure and temperature are acquired by a data acquisition system driven by a personal computer (PC). Hydrate formation experiments are conducted in a semibatch manner at constant pressure and temperature. The gas from the SV is supplied continuously into the CR to ensure the constant pressure of the CR.

2.2. Materials. The CH_4 and N_2 mixture gas with 50 mol % CH_4 supplied by Guangdong South China Special Gases Technology Institute Ltd., China, was used to model the drainage CBM. THF with a purity of 99.9% was supplied by Tianjin Kermel Chemical Reagent Co., Ltd., China. SDS with a purity of 99.9% was supplied by Tianjin Fuchen Chemical Reagent Co., Ltd. The deionized water was obtained by an ultrapure water system with a resistivity of 18.25 mΩ·cm^{-1} made by Nanjing Ultrapure Water Technology Co., Ltd., China. GC522 gas chromatography (GC) was supplied by Shanghai Wu Feng Scientific instrument Co., Ltd.

2.3. Procedures. In this work, all hydrate formation experiments are carried out in a semibatch manner with 180 mL volume of solution and a continuous supply of gas at constant pressure and temperature. The experimental procedure of hydrate formation and separation experiment is similar to that of recovering CO_2 from flue or fuel gas.[12] In the experiments, the 1.0 mol % THF solutions with different mass concentration of SDS (0, 250, 300, 500, 1000 ppm) are used. (1) Before doing the experiment, the CR is cleaned using deionized water and dried. Then, the 180 mL solution prepared with a desired concentration is introduced into the CR for each experiment. Subsequently, the CR with the solution is flushed with the CH_4/N_2 gas mixture at least four times to ensure that is air-free, and then the CH_4/N_2 gas mixture is charged into the cell for the desired initial operating pressure. (2) Once the temperature is stabilized, the magnetic stirrer in the CR is started at the speed of 500 rpm and the experimental time also begins to be recorded as 0. As the gas in the CR is consumed on account of the hydrate formation, high pressure gas automatically flows from the SV into the CR to maintain the constant operating pressure through the proportional–integral–derivative (PID) control system. During the experiment, the temperature and pressure in the system are recorded by a PC automatically. (3) After the system pressure is maintained constant for more than half an hour, the hydrate formation is considered to be completed. The magnetic stirrer is stopped, and the residual gas is sampled and analyzed with GC. Moreover, the change of moles of gas consumption in the CR (gas uptake) with time (t) can be calculated by the equation given by Linga et al.[18] The moles of the gas uptake (Δn_H) can be expressed as follows:

$$\Delta n_H = n_{H,0} - n_{H,t} = \left(\frac{PV}{zRT}\right)_{G,0} - \left(\frac{PV}{zRT}\right)_{G,t} + \left(\frac{PV}{zRT}\right)_{SV,0} - \left(\frac{PV}{zRT}\right)_{SV,t} \quad (1)$$

where z is the compressibility factor calculated by Pitzer's correlation.[30] The subscript t refers to time t. The subscript 0 refers to the initial time. The subscript G refers to the gas phase in the crystallizer. The subscript SV refers to the gas phase in the supply vessel. (4) After the end of hydrate formation, the pressure in the CR is quickly depressurized to atmospheric pressure, and then, it is closed. Thus, the hydrate is allowed to dissociate completely by heating to 293.15 K. Subsequently, the gas, which evolved from the decomposed hydrate and was released from the solution, is collected in the CR, and the composition of the decomposed gas phase is determined by GC.

Prior to commencing the separation experiment, one cycle of hydrate formation and decomposition is carried out to ensure the memory effect. The solution with the memory effect can obviously shorten the induction time of the hydrate formation.[31]

2.4. CH_4 Separation Efficiency. The separation efficiency can be determined by the CH_4 recovery or split fraction (S.Fr.) and CH_4 separation factor (S.F.), which can be obtained according to the following equations.[17,32]

$$\text{S.Fr.} = \frac{n^H_{CH_4}}{n^{feed}_{CH_4}} \quad (2)$$

$$\text{S.F.} = \frac{n^H_{CH_4} n^G_{N_2}}{n^H_{N_2} n^G_{CH_4}} \quad (3)$$

where $n^{feed}_{CH_4}$ is defined as the moles of CH_4 in the feed gas. $n^H_{CH_4}$ and $n^G_{CH_4}$ are the moles of CH_4 in the hydrate and gas phases, respectively. $n^H_{N_2}$ and $n^G_{N_2}$ are the moles of N_2 in the hydrate and gas phases, respectively.

dx.doi.org/10.1021/ef201804d | Energy Fuels 2012, 26, 1144–1151

3. RESULTS AND DISCUSSION

In this work, a total of nine experimental runs were carried out to investigate the CH_4 separation efficiencies of hydrate formation at the different conditions, including the fresh and memory water (runs 3 and 4), the different SDS concentrations in the 1.0 mol % THF aqueous solution (runs 1, 2, 4, 5, and 6) and the different initial operating pressure (runs 4, 7, 8, and 9), to find the optimal operating conditions for recovering and concentrating CH_4 from the drainage CBM via hydrate formation. Table 1 summarizes the results from the separation experiments with the different conditions.

3.1. Memory Effect. Memory refers to the situation where water that is used in the experiments has experienced hydrate formation.[33] As a typical case, Figure 2 gives the moles of gas consumed (amount of gas uptake) for hydrate formation in the presence of the 300 ppm SDS in the 1.0 mol % THF aqueous solution with fresh and memory water at 279.15 K and 3.50 MPa for runs 3 and 4. It can be seen from Figure 2 that the time corresponding to point A is the induction time in the memory water and that corresponding to point B is the induction time in the fresh water. The explanation for this can be given elsewhere.[14] As shown in Figure 2, the induction time in the memory water (2.3 min) is approximately a third as long as that in the fresh water (7.2 min) due to the memory effect. It can also be seen from Figure 2 that the moles of gas uptake with the fresh and memory water increase gradually in the processes of the hydrate formation and reach the plateau after approximately 2.0 and 2.5 h, respectively. It may be due to the fact that the gas hydrate forms substantially and agglomerates at the gas/liquid interface as the experiments progress. Extensive hydrate formation and crystal agglomeration result in the accumulation of crystals as stagnant pockets at the gas/water interface which prevents more gas from coming into contact with the water. The similar phenomenon can be found elsewhere.[31] In addition, it is also shown in Figure 2 that the final amount of the gas uptake obtained from the memory water (0.1682 mol) is approximately 12% higher than that obtained from the fresh water (0.1501 mol). Figure 3 gives the CH_4 concentration in decomposed gas phase, the CH_4 split fraction, and the CH_4 separation factor for 1.0 mol % THF aqueous solution in the presence of 300 ppm SDS with the fresh water and memory water at 279.15 K and 3.50 MPa. As shown in Figure 3, the CH_4 concentration in the decomposed gas phase, the CH_4 split fraction, and the CH_4 separation factor with the memory water, approximately 65 mol %, 82%, and 3.34, are higher than those with the fresh water, approximately 58 mol %, 78%, and 2.17, respectively. Hence, the memory water is more abstractive and effective for the CH_4 recovery from the CH_4/N_2 gas mixture in the application in industry. Actually, using the memory water circularly to recover CH_4 from the drainage CBM meets also the requirement of the operational process in industry. Thus, the following experiments are carried out in the memory water.

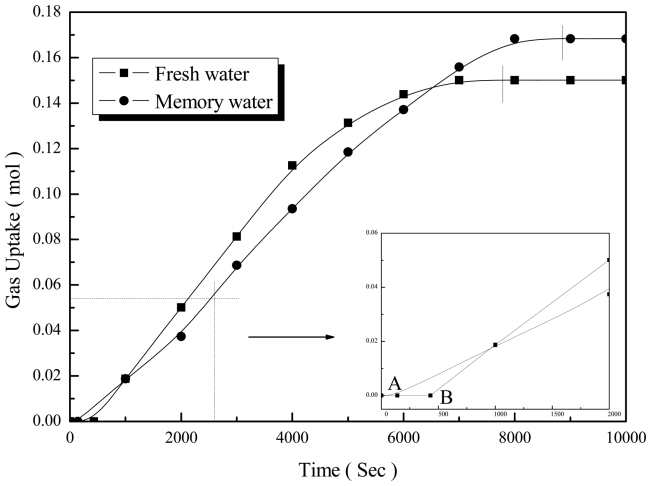

Figure 2. Gas uptake curves for 1.0 mol % THF aqueous solution in the presence of 300 ppm SDS with fresh and the memory water at 279.15 K and 3.50 MPa for runs 3 and 4.

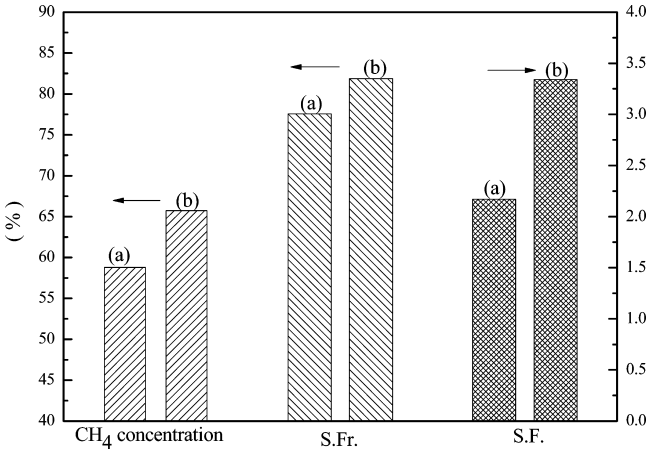

Figure 3. CH_4 concentration in decomposed gas phase, CH_4 split fraction (S.Fr.), and CH_4 separation factor (S.F.) for 1.0 mol % THF aqueous solution in the presence of 300 ppm SDS with the fresh water (a) and memory water (b) at 279.15 K and 3.50 MPa.

3.2. Effect of SDS Concentration. Figure 4 shows the change of gas uptakes for hydrate formation in the 1.0 mol % THF aqueous solutions in the presence of SDS with the different concentrations at 279.15 K and 3.50 MPa for runs 1, 2, 4, 5, and 6. As seen, the hydrate formation rate in the initial stage of the hydrate formation process is high and, then, reduces gradually. Eventually, the hydrate formation rate for runs 1, 2, 4, 5, and 6 has little change after approximately 3.1,

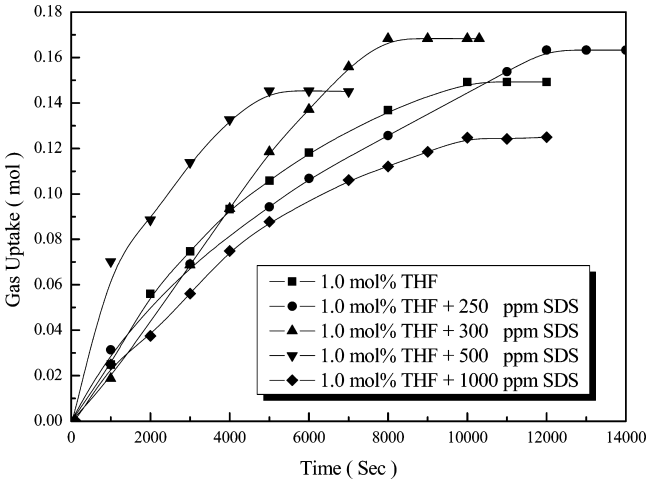

Figure 4. Gas uptake measurements for five experiments conducted at 3.50 MPa and 279.15 K in the systems with different SDS concentrations (0, 250, 300, 500, 1000 ppm) for runs 1, 2, 4, 5, and 6.

dx.doi.org/10.1021/ef201804d | Energy Fuels 2012, 26, 1144–1151

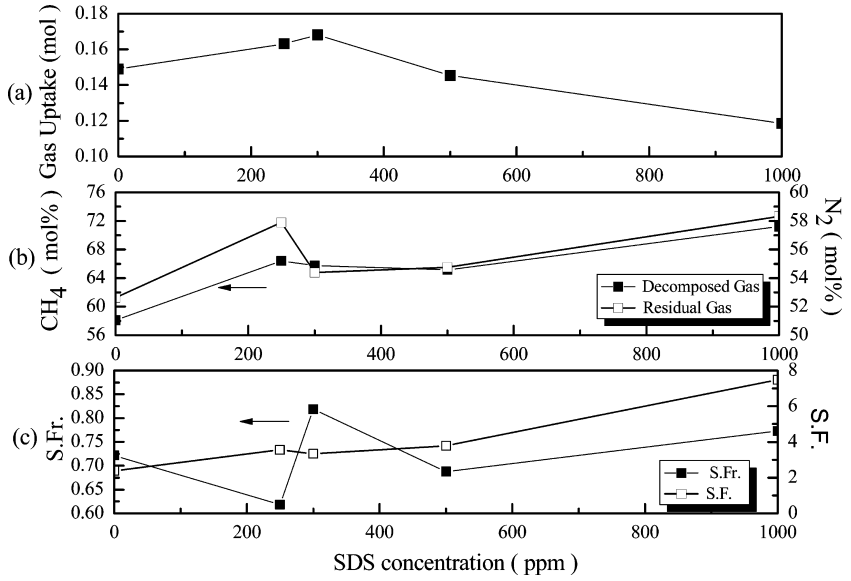

Figure 5. Hydrate formation from systems with 1.0 mol % THF solution in the presence of 0−1000 ppm SDS at 279.15 K and 3.50 MPa: (a) the gas uptake, (b) N_2 concentration in residual gas, and CH_4 concentration in decomposed gas phase and (c) CH_4 split fraction (S.Fr.) and CH_4 separation factor (S.F.).

3.6, 2.2, 1.7, and 3.0 h, respectively. The reason for this is explained in Figure 2. In addition, from Figures 4 and 5a, it can be found that the maximum of the gas uptake (0.1682 mol) can be obtained in the system with 300 ppm SDS and the minimum (0.1185 mol) can be obtained in the system with 1000 ppm SDS.

It is noted that the final amount of gas uptake presents an increasing trend for the systems with SDS concentration from 0 to 300 ppm. However, the final amount of gas uptake reduces with the increase of SDS concentration from 300 to 1000 ppm. As seen from Table 1 and Figure 5a, the final amount of the gas uptake in the system with 250 ppm SDS is 0.1632 mol and it is enhanced 9.5% relative to the system without SDS (0.1490 mol). The final amount of the gas uptake in the system with 300 ppm SDS is up to 0.1682 mol, which is 12.9% higher than that in the system without SDS. In addition, it is found that the final amount of the gas uptake in the system with 1000 ppm SDS is 0.1185 mol, and it is decreased by approximately 21% relative to that in the system without SDS. The differences of the gas uptakes in the systems with various SDS concentrations are because of the characteristics of SDS as a surfactant in the solution. We fitted the critical micelle concentration (CMC) data of SDS at different temperatures given by the literature[34−37] and determined that the CMC of SDS at 279.15 K is approximately 350 ppm in the work. Thus, the SDS concentration of 300 ppm is slightly lower than its CMC and that of 500 ppm is higher than its CMC. When the SDS concentration is lower than CMC, with the increase of the SDS concentration, DS^- monomers in the solution gradually accumulate on the gas/liquid surface, gradually form the DS^- monomolecular film, and, thus, cause the gradual decrease of the surface energy, i.e., the gradual decrease of the surface tension. When the SDS concentration is equal to the CMC, the DS^- monomolecular film is saturated by DS^- monomers. At the time, the surface tension is lowest. When the SDS concentration is higher than CMC, the DS^- monomers exist in the solution in the form of the micelles. During the period, the system surface tension remains the lowest value and has no change. Therefore, the surface tension in the system with the SDS concentration of 300 ppm is smaller than that in the system with the SDS concentration of 250 ppm. Consequently, the lower surface tension, which means lower surface energy, leads to the gas dissolving in the solution more easily. Hence, the final amount of gas uptake in the system with 300 ppm SDS is higher than that in the system with 250 ppm SDS. However, when the SDS concentration is higher than its CMC, with the increase of the DS^- micelles, more crystal nucleuses for hydrate formation are bundled in the hydrophobic domains formed by adsorbed DS^- monomers and the contact of gas and hydrate crystal nucleuses is frustrated to form more hydrates.[31] Thus, the gas uptake reduces as the SDS concentration increases from 500 to 1000 ppm.

In addition, as shown in Figure 5b, the CH_4 concentrations in the decomposed gas phase obtained from the systems with SDS are higher than that obtained from the system without SDS (approximately 58 mol %). This indicates that DS^- monomers are favorable for forming the CH_4 hydrate preferentially in THF solutions. This may be attributed to the existence of the DS^- monomolecular film and the abundant SDS micelles in solutions, which make the CH_4 molecules go into the solution more easily than the N_2 molecules because CH_4 and DS^- have similar alkyl radical structures. Also, it can be seen from Figure 5b that the CH_4 concentration in the decomposed gas phase at the SDS concentration of 250 ppm (less than CMC) is slightly higher than that at the SDS concentrations of 300 ppm (close to CMC) and has little change in the SDS concentration range from 300 to 500 ppm. Subsequently, the CH_4 concentration has a relatively large increase with the SDS concentration changes from 500 to 1000 ppm. The reason is not very clear. This requires our further research in the future work. The N_2 concentration in the residual gas phase has the similar change trend with the CH_4 concentration in decomposed gas phase as the SDS concentration increases from 0 to 1000 ppm.

The CH_4 separation factor indicates the separation ability of recovering CH_4 from the CH_4/N_2 gas mixture. Figure 5c shows the changes of the CH_4 separation factor with the increase of SDS concentration at 279.15 K and 3.50 MPa after one-stage

dx.doi.org/10.1021/ef201804d | *Energy Fuels* 2012, 26, 1144−1151

hydrate-based separation. Moreover, it has a similar change trend with the CH_4 concentrations in the decomposed gas phase with the increase of SDS concentration. Thus, the experimental results indicate that the CH_4 separation factors in the systems with SDS are higher than that in the system without SDS (approximately 2.4). This proves that SDS has a positive influence on the recovery of CH_4 from the CH_4/N_2 gas mixture via hydrate formation. It can be seen in Figure 5c that the CH_4 separation factor only changes by approximately 0.2 with the increase of SDS concentration from 250 to 500 ppm. However, when the SDS concentration is 1000 ppm, the CH_4 separation factor is twice as high (up to approximately 7.5) than that in the SDS concentration range of 250−500 ppm. This possibly results from the existence of the abundant SDS micelles in systems with 1000 ppm SDS. Thus, the addition of SDS is also helpful to enhance the CH_4 recovery ability from the CH_4/N_2 gas mixture with the hydrate-based separation technology.

Generally, the CH_4 split fraction is another significant parameter in the industrial application. A separation process with a higher CH_4 split fraction value can produce more products. Consequently, a bigger economic benefit can be obtained. Figure 5c also gives the change of the CH_4 split fraction vs the SDS concentration at 279.15 K and 3.50 MPa after one-stage hydrate-based separation. The experimental results indicate that the maximum of the CH_4 split fraction (81.87%) obtained in the system with 300 ppm SDS is approximately 10% higher than that obtained in the system without SDS (72.18%). Furthermore, the minimum of the CH_4 split fraction (61.82%) is obtained in the system with 250 ppm SDS. It illustrates that the maximum of the CH_4 split fraction can be obtained when the SDS concentration is near its CMC value.

Thus, as seen from Figures 4 and 5, the experimental results indicate that the system with SDS can effectively recover CH_4 from the CH_4/N_2 gas mixture via hydrate formation. Hence, it is determined that the system with 300 ppm SDS in 1.0 mol % THF aqueous solution is the optimal system to recover CH_4 from the CH_4/N_2 gas mixture via hydrate formation by considering comprehensively the CH_4 separation factor and the CH_4 split fraction along with the hydrate formation rate, the amount of the gas uptake, and the CH_4 concentration in the decomposed gas phase. Thus, the following experiments are carried out in the 1.0 mol % THF aqueous solution in the presence of 300 ppm SDS.

3.3. Effect of Initial Operating Pressure. The influences of the different initial operating pressures (1.50, 2.50, 3.50, and 4.50 MPa) on the gas uptakes, the CH_4 concentrations in decomposed gas phases, the CH_4 split fractions, and the CH_4 separation factors are investigated in the system with 300 ppm SDS at 279.15 K for runs 4, 7, 8, and 9. As shown in Figure 6, the amount of the gas uptake increases with the increase of the initial operating pressure from 1.50 to 3.50 MPa. It may be attributed to the fact, on the one hand, that the higher initial operating pressure makes more gas go into the THF aqueous solution and furthermore causes more gas hydrate to form, resulting in more gas consumed; on the other hand, the increase of the amount of gas going into the solution correlates with the enhancement of the gas hydrate growth rate, which also means the enhancement of the gas consumption rate. However, the amount of gas uptake at 4.50 MPa is slightly smaller than that at 3.50 MPa. This may be due to the fact that the gas hydrate forms substantially and agglomerates at the gas/liquid interface when the initial operating pressure is relatively high. Extensive hydrate formation and crystal agglomeration results in the accumulation of crystals as stagnant pockets at the gas/water interface which prevents more gas from coming into contact with the water. Thus, more agglomeration results in a smaller amount of gas in the solution for hydrate formation. It can be seen in Figure 7a that the maximum amount of gas uptake at 3.50 MPa is 0.1682 mol, which is slightly higher than the final amount of gas uptake at 4.50 MPa (0.1636 mol). In addition, the final amount of gas uptake at 3.50 MPa is twice that at 1.50 MPa (0.0808 mol).

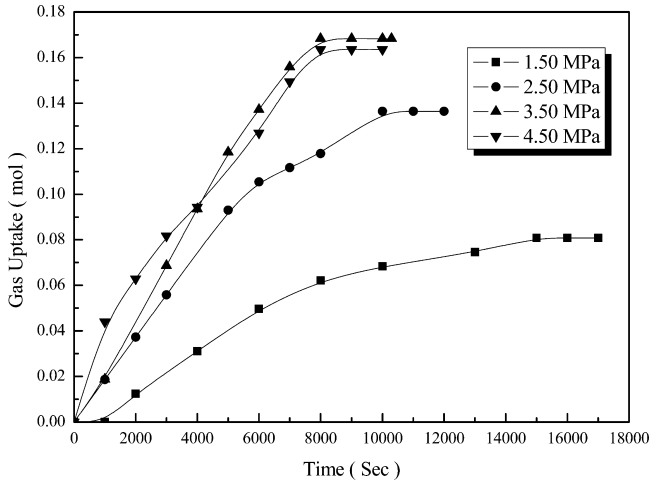

Figure 6. Gas uptake measurements for four experiments conducted at 279.15 K and different initial operating pressures (1.50, 2.50, 3.50, and 4.50 MPa) in the systems with 1.0 mol % THF solution in the presence of 300 ppm SDS for runs 4, 7, 8, and 9.

It can be seen from Figure 6 that the hydrate formation rates slow down and reach the individual plateau after approximately 4.56, 3.19, 2.22, and 2.20 h at 1.50, 2.50, 3.50, and 4.50 MPa, respectively. Similar behaviors were observed for runs 1−6. Generally, the hydrate formation rates at 3.50 and 4.50 MPa are higher than those at 1.50 and 2.50 MPa. In addition, the reaction time at 3.50 and 4.50 MPa shortens by approximately 2 h, compared with that at 1.50 MPa.

Figure 7b shows the changes of the N_2 concentration in the residual gas phase and the CH_4 concentration in the decomposed gas phase at the initial operating pressure range from 1.50 to 4.50 MPa in 1.0 mol % THF aqueous solution in the presence of 300 SDS after one-stage hydrate-based separation at 279.15 K. As seen, they all decrease with the increase of the initial operating pressure. It is noted that the higher initial operating pressure can not entrap more of the CH_4 molecules in the hydrate slurry phase. As seen in Figure 7b, the N_2 concentrations in the residual gas phase decrease from 61.57 mol % at 1.50 MPa to 54.39 mol % at 3.50 MPa and the CH_4 concentrations in the decomposed gas phase decrease from 70.59 mol % at 1.50 MPa to 64.35 mol % at 4.50 MPa. Moreover, as shown in Figure 7c, the CH_4 split fraction shows a similar reduction trend with the increase of initial operating pressure and achieves the biggest value of approximately 90% when the initial operating pressure is 1.50 MPa. In fact, the above change characteristics can be explained by the different selectivity of CH_4 and N_2 in the hydrate formation process with the different initial operating pressures. In comparison to the N_2 molecules, the CH_4 molecules are preferential to form the CH_4 hydrate at a lower initial operating pressure; however, the

dx.doi.org/10.1021/ef201804d | Energy Fuels 2012, 26, 1144−1151

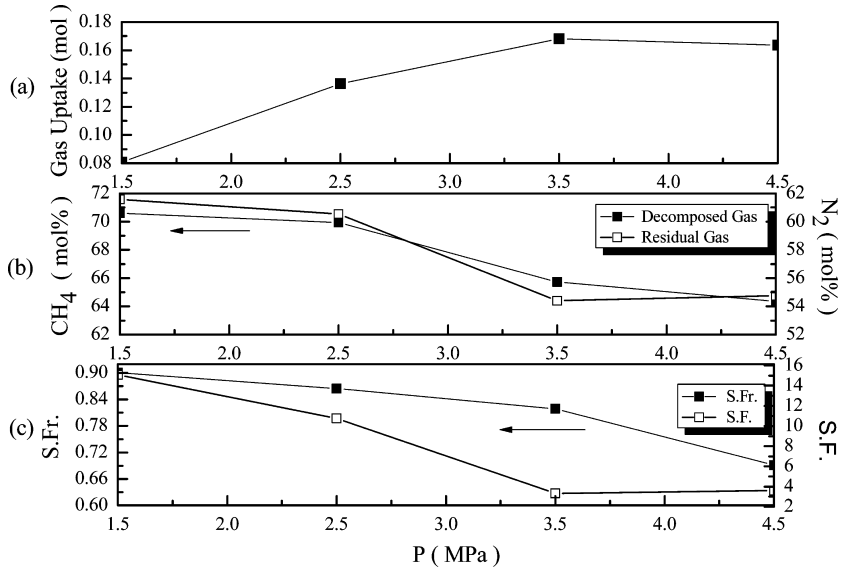

Figure 7. Hydrate formations from systems with 1.0 mol % THF in the presence of 300 ppm SDS at 279.15 K and different initial operating pressures: (a) the gas uptake, (b) N_2 concentration in the residual gas and CH_4 concentration in the decomposed gas phase, and (c) CH_4 split fraction (S.Fr.) and CH_4 separation factor (S.F.).

N_2 molecules can begin to compete with the CH_4 molecules for hydrate cage (5^{12}) occupancy with a higher initial operating pressure, resulting in the decrease of the CH_4 concentration in the decomposed gas phase, and the CH_4 split fraction decreases with increasing the initial operating pressure.

As shown in Figure 7c, the CH_4 separation factor decreases from 15.08 to 3.44 with the increase of the initial operating pressure from 1.50 to 3.50 MPa, and it is 10.77 when the initial operating pressure is 2.50 MPa. However, it is 3.60 when the initial operating pressure is 4.50 MPa. This illustrates that the low initial operating pressure at 1.50 and 2.50 MPa have better separation ability for recovering CH_4 from CH_4/N_2 gas mixture than that at 3.50 and 4.50 MPa. Hence, it is unfavorable for recovering CH_4 from CH_4/N_2 gas mixture with the high initial operating pressures.

Generally, it can be seen from the above analysis, the lower initial operating pressure can result in the higher N_2 concentration in residual gas phase, CH_4 concentration in decomposed gas phase, the CH_4 separation factor, and CH_4 split fraction. However, it can be seen from Figures 6 and 7a that the hydrate formation rate and the final amount of the gas uptake at 1.50 MPa are too low to be feasible in industry. Therefore, it is necessary to determine an appropriate initial operating pressure for the separation process. It can be found from Figure 7 that the values of the N_2 concentration in the residual gas phase, the CH_4 concentration in the decomposed gas phase, the CH_4 split fraction, and the CH_4 separation factor at 2.50 MPa are 60.54 mol %, 69.93 mol %, 86.44%, and 10.77, respectively. They are slightly less than those at 1.50 MPa, which are 61.57 mol %, 70.59 mol %, 90.05%, and 15.08, respectively. Hence, it is determined that the initial operating pressure of 2.50 MPa is the optimal condition for recovering CH_4 from the CH_4/N_2 gas mixture in the system in the presence of 300 ppm SDS in the 1.0 mol % THF aqueous solution by considering comprehensively the amount of the gas uptake, the hydrate formation rate, the CH_4 concentration in the decomposed gas phase, the N_2 concentration in the residual gas phase, and the CH_4 split fraction and separation factor.

4. CONCLUSIONS

In this work, the optimal operating condition and the corresponding CH_4 separation efficiency for recovering CH_4 from the CH_4/N_2 gas mixture via hydrate formation were investigated in the 1.0 mol % THF aqueous solution at 279.15 K. It is found that the memory water has an advantage to recover CH_4 from the CH_4/N_2 gas mixture. The system with the SDS concentration nearby CMC and the operating conditions with low initial operating pressure are helpful to recover CH_4 and can enhance the separation efficiency. However, the amount of the gas uptake is low in the system with SDS concentration above 300 ppm or at 1.50 MPa. Thus, the 1.0 mol % THF aqueous solution in the presence of 300 ppm SDS with the initial operating pressure of 2.50 MPa is the optimal for the CH_4 separation purpose. Under these conditions, the final amount of gas uptake, the CH_4 concentration in the decomposed gas phase, and the CH_4 split fraction and separation factor after the one-stage hydrate-based process are 0.1364 mol, 69.93 mol %, 86.44%, and 10.77, respectively. Thus, the data illustrate the conceptual process that CH_4 in drainage CBM can be recovered efficiently via hydrate-based separating technology at mild conditions in industry.

AUTHOR INFORMATION

Corresponding Author

*Telephone: +86-20-87057037. Fax: +86-20-87034664. E-mail: lixs@ms.giec.ac.cn.

Notes

The authors declare no competing financial interest.

ACKNOWLEDGMENTS

The authors gratefully appreciate financial support from the National Natural Science Foundation of China (50874098 and 51076155) and Science & Technology Program of Guangdong Province (2009B050600006).

REFERENCES

(1) *Petroleum. Feasibility study of coal bed methane production in China*, A technology report for the EU-China Energy and Environment Programme funded by the European Union and the National Development and Reform Commission of China (EuropeA/120723/D/SV/CN). 2008.

(2) Tang, P. C.; Yang, S. Y.; et al. The accurnulation mechanismic research of coal-bed methane reservoir. *Chin. Min. Mag.* **2009**, *18* (2), 94−97.

(3) Shi, H. N.; Mei, Y. G.; et al. Research an application of intelligent recovery technology for Fanzhuang high rank CBM wells. *Oil Drilling Prod. Technol.* **2010**, *32* (4), 107−111.

(4) Chen, Y. P.; Wang, Y. B.; et al. Optimization of casing program san its application to CBM pinnate horizontal well. *Oil Drilling Prod. Technol.* **2010**, *32* (4), 81−85.

(5) Liang, W. G.; W., D.; Zhao, Y. S. Experimengtal study of coalbeds methane replacement by carbon dioxide. *Chin. J. Rock Mechan. Eng.* **2010**, *29* (4), 665−673.

(6) Xu, C. H.; Z., G.; Long, S. X.; et al. The new technology analysis of improving the coalbed methane recovery. *Explor. Tech.* **2009**, 51−72, DOI: 10.3969/j.issn.1672-7703.

(7) Pilcher, R. C.; C. M., M.; Collings, R. C.;et al. Recent trends in recovery & use of coal mine methane. *The 3rd international conference of pollution-reducing technology of methane and nitrous oxide*, Bejing, Nov. 6−7, 2003; pp 5−122.

(8) Kerr, T.; Yang, M. *Coal mine methane in China: A budding asset with the potential to bloom*, An assessment of technology, policy and financial issues relating to CMM in China, based on interviews conduced at coal mines in Guizhou and Sichuan Provinces, International Energy Agency, 2009.

(9) Guo, P.; L., M. Research progress of separation of CH_4/N_2 in coal-bed methane. *Chem. Ind. Eng. Progress* **2008**, *27* (7), 963−967.

(10) Li, X. S.; Xu, C. G.; Chen, Z. Y.; Wu, H. J. Hydrate-based pre-combustion carbon dioxide capture process in the system with tetra-n-butyl ammonium bromide solution in the presence of cyclopentane. *Energy* **2011**, *36* (3), 1394−1403.

(11) Zhang, Y.; Wu, H. J.; Li, X. S.; Chen, Z. Y.; Li, G.; Zeng, Z. Y. Dissociation behavior of methane hydrate in porous media. *Chem. J. Chin. Univ.* **2010**, *31* (9), 1848−1854.

(12) Li, X. S.; Xu, C. G.; Chen, Z. Y.; Wu, H. J. Tetra-n-butyl ammonium bromide semi-clathrate hydrate process for post-combustion capture of carbon dioxide in the presence of dodecyl trimethyl ammonium chloride. *Energy* **2010**, *35* (9), 3902−3908.

(13) Li, X. S.; Xia, Z. M.; Chen, Z. Y.; Yan, K. F.; Li, G.; Wu, H. J. Equilibrium hydrate formation conditions for the mixtures of CO(2) + H(2) + tetrabutyl ammonium bromide. *J. Chem. Eng. Data* **2010**, *55* (6), 2180−2184.

(14) Li, X. S.; Xia, Z. M.; Chen, Z. Y.; Yan, K. F.; Li, G.; Wu, H. J. Gas hydrate formation process for capture of carbon dioxide from fuel gas mixture. *Ind. Eng. Chem. Res.* **2010**, *49* (22), 11614−11619.

(15) Kang, S. P.; Lee, H. Recovery of CO_2 from Flue Gas Using Gas Hydrate: Thermodynamic Verification through Phase Equilibrium Measurements. *Environ. Sci. Technol.* **2000**, *34* (20), 4397−4400.

(16) Klara, S. M.; Srivastava, R. D. U.S. DOE integrated collaborative technology development program for CO_2 separation and capture. *Environ. Progr.* **2002**, *21* (4), 247−253.

(17) Linga, P.; Kumar, R.; Englezos, P. The clathrate hydrate process for post and pre-combustion capture of carbon dioxide. *J. Hazard. Mater.* **2007**, *149* (3), 625−629.

(18) Linga, P.; Kumar, R.; Englezos, P. Gas hydrate formation from hydrogen/carbon dioxide and nitrogen/carbon dioxide gas mixtures. *Chem. Eng. Sci.* **2007**, *62* (16), 4268−4276.

(19) Happel, J.; Hnatow, M. A.; Meyer, H. The study of separation of nitrogen from methane by hydrate formation using a novel apparatus. *International Conference on Natural Gas Hydrates*, New York, June 20−24, 1994; Vol. *715*, pp 412−424.

(20) Xu, F.; Wu, Q.; Zhu, L. H. Fractal-like Kinetic Characteristics of Coalbed Methane Hydrate Dissociation at Normal Pressure. *Chin. J. Chem.* **2011**, *29* (1), 21−26.

(21) Zhao, J. Z.; Zhen, Y. S.; Shi, D. X. Experiment on methane concentration from oxygen-containing coal bed gas by THF solution hydrate formation. *J. Chin. Coal Soc.* **2008**, *33* (12), 1419−1424.

(22) Zhang, B. Y.; Wu, Q. Thermodynamic promotion of tetrahydrofuran on methane separation from low-concentration coal mine methane based on hydrate. *Energy Fuels* **2010**, *24*, 2530−2535.

(23) Sun, Q.; X., G.; Liu, A. X.; et al. Experimental study on the separation of CH_4 and N_2 via hydrate formation in TBAB solution. *Ind. Eng. Chem. Res.* **2011**, *50*, 2284−2288.

(24) Wu, Q.; He, X. Q.; Zhang, B. Y.; Wang, Y. J. Thermodynamic effect of surfactant on gas hydrate formation. *J. Chem. Ind. Eng. (Chin.)* **2006**, *57* (12), 2793−2797.

(25) Zhang, B. Y.; Wu, Q. Dynamic Effect of Surfactant on Gas Hydrate Formation Process. *J. Chin. Univ. Mining Technol.* **2007**, *36* (4), 478−481.

(26) Feng, X.; WU, Q.; Zhang, B. Y. Study on Storage and Transportation of Coalbed Methane Based on Hydrate Technology. *Gas Heat* **2008**, *28* (6), 39−43.

(27) Adisasmito, S.; Frank, R. J.; Sloan, E. D. Hydrates of carbon-dioxide and methane mixtures. *J. Chem. Eng. Data* **1991**, *36* (1), 68−71.

(28) Vancleeff, A.; Diepen, G. A. M. Gas hydrates of nitrogen and oxygen. *Recueil Des Travaux Chimiques Des Pays-Bas—J. R. Netherlands Chem. Soc.* **1960**, *79* (5), 582−586.

(29) Jhaveri, J.; Robinson, D. B. Hydrates in methane-nitrogen system. *Can. J. Chem. Eng.* **1965**, *43* (2), 75−&.

(30) Smith, J. M.; Van Ness, H. C.; Abbott, M. M. *Introduction to chemical engineering thermodynamics*; McGraw-Hill: New York, 2001.

(31) Cai, J.; Chen, Z. Y.; Li, X. S.; Xu, C. G., Separation and purification of methane from coal-bed methane via the hydrate technology. In *2010 International Conference on Energy and Environment Technology, 2010 International Conference on Digital Manufacturing & Automation*, Changsha, China, Dec. 18−20, 2010; Vol. *2*, pp 341−345.

(32) Englezos, P.; Linga, P.; Adeyemo, A. Medium-pressure clathrate hydrate/membrane hybrid process for postcombustion capture of carbon dioxide. *Environ. Sci. Technol.* **2008**, *42* (1), 315−320.

(33) Lee, J. D.; Susilo, R.; Englezos, P. Kinetics of structure H gas hydrate. *Energy Fuels* **2005**, *19* (3), 1008−1015.

(34) Linga, P.; Kumar, R.; Lee, J. D.; Ripmeester, J.; Englezos, P. A new apparatus to enhance the rate of gas hydrate formation: Application to capture of carbon dioxide. *Int. J. Greenhouse Gas Control* **2010**, *4* (4), 630−637.

(35) Zhong, Y.; Rogers, R. E. Surfactant effects on gas hydrate formation. *Chem. Eng. Sci.* **2000**, *55* (19), 4175−4187.

(36) Sun, Z. G.; Wang, R. Z.; Ma, R. S.; Guo, K. H.; Fan, S. S. Natural gas storage in hydrates with the presence of promoters. *Energy Conver. Manage.* **2003**, *44* (17), 2733−2742.

(37) Lee, J. W.; Zhang, J. S.; Lo, C.; Somasundaran, P. Competitive adsorption between SDS and carbonate on tetrahydrofuran hydrates. *J. Colloid Interface Sci.* **2010**, *341* (2), 286−288.

(38) Kim, S. M.; Lee, J. D.; Lee, H. J.; Lee, E. K.; Kim, Y. Gas hydrate formation method to capture the carbon dioxide for pre-combustion process in IGCC plant. *Int. J. Hydrogen Energy* **2011**, *36*, 1115−1121.